JOC The Journal of Organic Chemistry

Featured Article

pubs.acs.org/joc

"Catch-and-Release" of HNO with Pyrazolones

Daryl A. Guthrie, Anthony Ho, Cyrus G. Takahashi, Anthony Collins, Matthew Morris, and John P. Toscano*

Department of Chemistry, 3400 North Charles Street, Johns Hopkins University, Baltimore, Maryland 21218, United States

Supporting Information

ABSTRACT: A new and versatile class of HNO donors, the (hydroxylamino)-pyrazolone (HAPY) series of HNO donors utilizing pyrazolone (PY) leaving groups, is described. HNO, the smallest *N*-based aldehyde equivalent, is used as a reagent along with a variety of PY compounds to synthesize the desired HAPY donors in what can be considered an *N*-selective HNO-aldol reaction in up to quantitative yields. The bimolecular rate constant of HNO with PY in pH 7.4 phosphate buffer at 37 °C can reach 8×10^5 M^{-1} s^{-1}. In ^{1}H NMR experiments, the HAPY compounds generate HNO quantitatively (trapped as a phosphine aza-ylide) with half-lives spanning 3 orders of magnitude (minutes to days) under physiologically relevant conditions. B3LYP/6-31G* calculations confirm the energetically favorable reactions between HNO and the PY enol and enolate, whereas HNO release is expected to occur through the oxyanion (*O*HN-PY) of each HAPY compound. HNO has been shown to provide functional support to failing hearts.

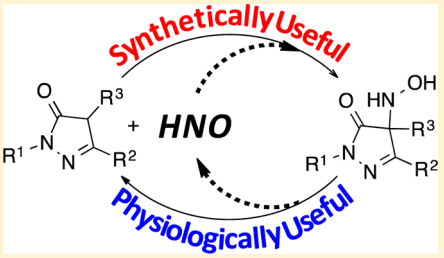

INTRODUCTION

Heart failure, defined as the inability of the heart to pump enough blood to supply the metabolic demands of the body, affects more than 23 million people worldwide with total annual costs in 2013 of $32 billion in the US alone.[1−3] Azanone (HNO), commonly referred to as nitroxyl, is the one-electron reduced and protonated form of nitric oxide (NO) and has been shown to improve both vasorelaxation and myocardial contractility, making it a promising alternative therapeutic in the fight against congestive heart failure.[4−8]

The practical use of HNO as a therapeutic agent is complicated due to its propensity to spontaneously dimerize ($k = 8 \times 10^6$ M^{-1} s^{-1}) to hyponitrous acid (HON═NOH), which dehydrates to give nitrous oxide (N_2O).[9] Thus, HNO donors, such as Angeli's salt ($Na_2N_2O_3$), have been utilized to discern the biological activity of HNO.[4−8] Angeli's salt has a relatively short half-life of ca. 2−3 min at pH 7.4, 37 °C[10] and produces HNO along with an equimolar amount of nitrite, which possesses its own biological activity.[11,12] Unfortunately, Angeli's salt is not ideal from a drug development perspective since derivatives that are HNO donors have yet to be successfully realized.

Identifying physiologically useful donor molecules that evolve HNO in a controlled and tunable fashion is an important and ongoing challenge for fundamental research and biomedical applications. Furthermore, sustained release of low concentrations of HNO might be an important step to mimic hypothesized endogenous HNO production.[13] In comparison, the availability of NO donors was invaluable to the elucidation of the biological properties and endogenous production of NO. Thus, new robust HNO donor platforms amenable to structure−activity relationship (SAR) studies designed to optimize both physiochemical and physiological properties are desired.

The most commonly used strategy for prolonging HNO release is through the use of ester prodrugs of otherwise efficient HNO donors. These include acyloxy nitroso compounds,[14,15] esters of primary amine-based diazeniumdiolates such as IPA/NO,[16−19] and precursors to acyl nitroso compounds[20−22] such as *N*,*O*-bis-acylated hydroxylamine derivatives.[23] The tunability of this strategy is reliant on the precursor ester hydrolysis rates, which can vary from seconds to hours. However, the overall chemistry of these long-acting HNO donors can be more complicated than is originally anticipated. For example, direct and HNO-mediated reactions of acyloxy nitroso compounds have been demonstrated with thiol-containing proteins;[24,25] dual mechanisms of HNO generation by IPA/NO-AcOM (*i*PrHN-N(O)═NO-CH_2OAc) and IPA/NO-aspirin can occur in the absence of esterase,[18,19] and optimization of HNO production from *N*,*O*-bis-acylated hydroxylamine derivatives requires the use of urea-based precursors with arenesulfonyl leaving groups in order to avoid both amide hydrolysis and acyl migration pathways.[23] Additionally, these precursors are all susceptible to esterase-mediated hydrolysis, which complicates drug development since esterase activity not only depends on the substrate but also shows strong interspecies, interorgan, and interindividual variability.[26]

Previously, we have reported the development of *N*-substituted hydroxylamines as efficient HNO donors based on the general formula (HOHN-X) where X is a good carbon-based leaving group.[27] The rate and amount of HNO released

Received: October 12, 2014
Published: January 16, 2015

DOI: 10.1021/jo502330w
J. Org. Chem. 2015, 80, 1338−1348

from these compounds is dependent mainly on the nature of the leaving group X. We identified examples from three independent hydroxylamine-substituted classes shown in Figure 1: (1) the hydroxylamino-Meldrum's acid (HAMA) class, (2) the (hydroxylamino)barbituric acid (HABA) class, and (3) the (hydroxylamino)pyrazolone (HAPY) class.

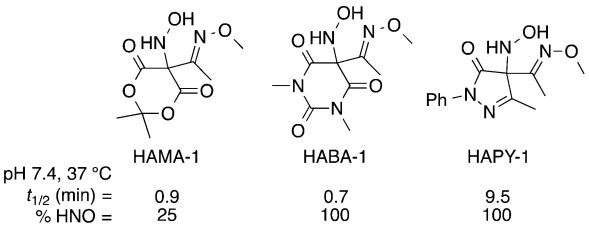

Figure 1. Previous examples from the HAMA, HABA, and HAPY classes of HNO donors.

Each example shares in common an *O*-methyloxime moiety attached to the carbon bearing the hydroxylamine group. Replacement of the *O*-methyloxime with simple alkyl groups on the HAMA and HABA scaffolds results in negligible HNO production following incubation at pH 7.4, 37 °C due to either competitive hydrolysis or rearrangement mechanisms of their ring core systems, respectively.[27] The hydrolysis pathway remains dominant in HAMA-1 even with *O*-methyloxime substitution, restricting further development of the HAMA class to examples with fast HNO release profiles. Strategies to curtail the non-HNO producing rearrangement pathway in the HABA class to favor HNO generation is the subject of a companion paper.[28]

On the other hand, the HAPY class of HNO donors (Scheme 1) offers several distinct advantages: (1) the

Scheme 1. General HNO Release from HAPY Class

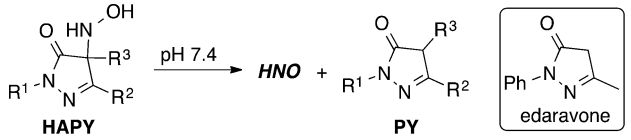

pyrazolone ring is expected to be resistant to hydrolysis and rearrangement, (2) multiple synthetic handles are available to investigate SAR, and (3) the byproducts are related to edaravone,[29−31] a potent antioxidant marketed in Japan to treat acute ischemic stroke, which has been reported to be effective for myocardial ischemia as well.

Herein, we are pleased to report the first series extension of the HAPY class of HNO donors by varying the groups at the R^1, R^2, and R^3 positions on the pyrazolone ring. In doing so, we have discovered a synthetically advantageous umpolung process in which the PY's 3-position switches from electrophilic to nucleophilic, thereby reducing the steps to the desired HAPY product from three to one. This discovery is made possible by recognizing that HNO can be viewed as an aldehyde equivalent. The phrase "catch-and-release" is thus attributed to describe the HAPY compounds' ability to undergo reversible generation of HNO. Because of this attribute, we have developed an ^{1}H NMR assay for the evaluation of half-life and HNO production in the presence of a phosphine-based trap for HNO to gauge how these donors might behave under physiological conditions where numerous biological targets for HNO exist.

RESULTS AND DISCUSSION

Early Studies. We first considered HAPY-2 (R^1 = phenyl, R^2 and R^3 = methyl), which was expected to generate HNO as shown in Scheme 1. This precursor was synthesized from the expected organic byproduct of HNO release, PY-2, which is structurally similar to edaravone and has comparable in vitro inhibitory activity with edaravone against lipid peroxidation.[31] PY-2 was readily prepared through the condensation of ethyl 2-methylacetoacetate and phenylhydrazine. Installation of the hydroxylamine group was accomplished analogously to the previously reported synthesis of HAPY-1 by formation of the corresponding bromide followed by reaction with *N*,*O*-bis(*tert*-butoxycarbonyl)hydroxylamine and subsequent acid deprotection (Scheme 2, path A).[27]

Scheme 2. Possible Synthetic Strategies: Traditional (Path A) vs Umpolung (Path B)

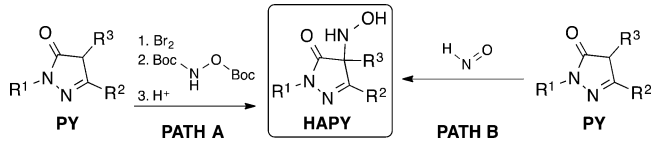

Previously, we examined HAPY-1 for HNO production in pH 7.4 phosphate-buffered saline at 37 °C by gas chromatographic headspace analysis to quantify the amount of its dimerization product, N_2O, as well as ^{1}H NMR spectroscopy to quantify the amount of the expected organic byproduct PY-1. HNO was confirmed as the source of N_2O for HAPY-1 by quenching with glutathione (GSH), a known efficient trap for HNO.[32,33]

Upon examination of HAPY-2, however, only trace amounts of N_2O are detected following 24 h incubation, and ^{1}H NMR analysis reveals that HAPY-2 is essentially stable. Interestingly, upon 24 h incubation with excess GSH (ca. 5 equiv), enhanced conversion of HAPY-2 to byproduct PY-2 is observed by ^{1}H NMR spectroscopy; the relative yield of PY-2 is 36%. Importantly, no other products arising from HAPY-2 are observed. Four conclusions can be drawn from these results: (1) the pyrazolone ring *is* stable against hydrolysis and rearrangement, (2) the decomposition rates of HAPY-1 and HAPY-2 differ dramatically, (3) HAPY decomposition may be reversible, and (4) an alternative means of monitoring HNO release in an expanded HAPY class is necessary.

Synthesis. We tested the possibility that PY-2 may be an efficient trap for HNO by monitoring the reaction of PY-2 and Angeli's salt in 10% D_2O, pH 7.4 phosphate buffer with the metal chelator, diethylenetriaminepentaacetic acid (DTPA), at room temperature by ^{1}H NMR spectroscopy (Figure 2). Consistent with our hypothesis, we observe the complete conversion of PY-2 to HAPY-2, which is the first example of what can be considered an *N*-selective nitroso-aldol reaction,[34−36] utilizing the smallest nitroso compound, HNO, as the reagent.

This new reactivity of HNO is not so unexpected given what has been reported in the literature. The chemical similarity between HNO and an aldehyde is greater than between HNO and an oxyacid.[9] In addition, HNO is a potent inhibitor of aldehyde dehydrogenase,[37,38] demonstrating its chemical similarity to acetaldehyde, though HNO is isoelectronic with formaldehyde. Pyrazolones, as well as other reactive enols and enolates, readily form aldol condensation products with

DOI: 10.1021/jo502330w
J. Org. Chem. 2015, 80, 1338−1348

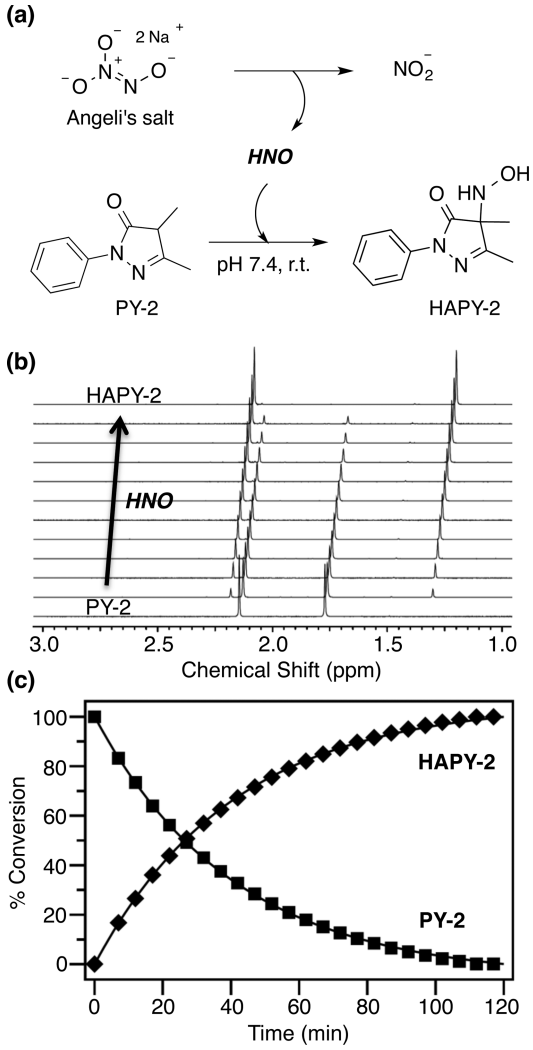

Figure 2. (a) *N*-Selective HNO–aldol reaction between PY-2 and Angeli's salt-derived HNO. (b) ^{1}H NMR spectra of the formation of HAPY-2 from PY-2 and Angeli's salt derived HNO in 10% D_2O, pH 7.4 phosphate buffer (0.25 M) with DTPA (0.2 mM) at room temperature. (c) Kinetics of the reaction using the integrated area of the upfield methyl group of PY-2 relative to the upfield methyl group of HAPY-2. The solid curves are calculated best fits to a single exponential function ($k = 4.0 \times 10^{-4}$ s^{-1} for each fit).

aldehydes in aqueous media.[39] Moreover, the nitroso-aldol reaction between carbonyl compounds and nitrosoarene and acyl nitroso compounds to produce enantioselective amines and alcohols following *N*–*O* bond reduction has been recently well documented.[34−36]

The reaction of HNO with PY to give HAPY is synthetically attractive, as it is the one-step umpolung strategy (Scheme 2, path B) to the traditional bromination–displacement–deprotection strategy (Scheme 2, path A). As such, we endeavored to find a useful preparatory procedure for this HNO–aldol reaction and apply it to an expanded HAPY class.

On the basis of the early studies comparing HAPY-1 and HAPY-2, a large variation in effective half-life is observed when the *O*-methyloxime group at the R^3 position of the pyrazolone ring is replaced with a methyl group. Moving forward, we probed the R^1 and R^2 positions with simple hydrogen, methyl, and substituted phenyl variations. Accordingly, PY-3–PY-12 (Table 1) were prepared (see the Experimental Section for synthetic procedures).

Table 1. HNO–Aldol Reaction of Pyrazolones

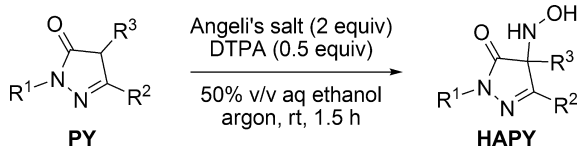

HAPY	R^1	R^2	R^3	% yield
1	Ph	Me	C(=NOMe)Me	74
2	Ph	Me	Me	89
3	Me	Me	C(=NOMe)Me	44
4	Me	Me	Me	76
5	H	Me	C(=NOMe)Me	35
6	H	Me	Me	75
7	4-ClPh	Me	Me	94
8	2-ClPh	Me	Me	96
9	Me	Ph	Me	89
10	Ph	Ph	Me	99
11	Me	4-ClPh	Me	99
12	Me	2-ClPh	Me	87

We have been able to develop a general synthetic protocol at room temperature that features the use of Angeli's salt, which has a suitable HNO generation rate for this procedure. An added advantage is that the nitrite byproduct is readily separated from the HAPY product. To initiate decomposition of Angeli's salt, DTPA was used as a proton source as well as to maintain a buffered solution (pH ≈ 8.0–8.5) and to preclude HNO reactivity with trace metals. A 50% v/v aqueous ethanol solution allowed both the organic and salt reagents to be readily soluble at typical reaction concentrations (0.1–0.4 M) (see the Experimental Section for details). The use of ethanol also aided in the preliminary drying steps by allowing the mild azeotropic removal of the water. This procedure is applicable for each HAPY example; the isolated synthetic yields are shown in Table 1. Further investigations are underway to render this process asymmetric.

Surprisingly, even the relatively efficient HNO donor, HAPY-1, can be isolated starting from PY-1 in better yield and in fewer steps when compared to the traditional bromination–displacement–deprotection strategy (one step, 74% vs three steps, 34% overall). The caveat here is that conversion to HAPY-1, or the other *O*-methyloxime derivatives HAPY-3 and HAPY-5, is not complete and requires the use of chromatographic separation to isolate. Fortunately, the respective isolated yields correspond well with the conversion yields, and under these reaction conditions, the HAPY products are relatively stable several hours after HNO generation from Angeli's salt has completed. Therefore, we believe the lower yields for these compounds are primarily due to less efficient trapping of HNO rather than the reactivity of the HAPY product. Otherwise, complete conversion was observed in the other HAPY examples, each equipped with a methyl group in the R^3 position, resulting in excellent isolated yields.

Kinetic Evaluation. Given the high conversion yields, particularly for the R^3 = methyl examples, we have quantified this reactivity of HNO with pyrazolones utilizing PY-2 as an example. We employed a competitive trapping experiment using the HNO donor, HABA-1, and tris(4,6-dimethyl-3-sulfanatophenyl)phosphine trisodium salt (TXPTS), another

DOI: 10.1021/jo502330w
J. Org. Chem. 2015, 80, 1338–1348

efficient and selective trap for HNO at pH 7.4, 37 °C (k_{TXPTS} = 9 × 10^5 M^{-1} s^{-1}) following Scheme 3.[40,41] HNO reacts with 2

Scheme 3. Competitive HNO Trapping Experiment at pH 7.4, 37 °C

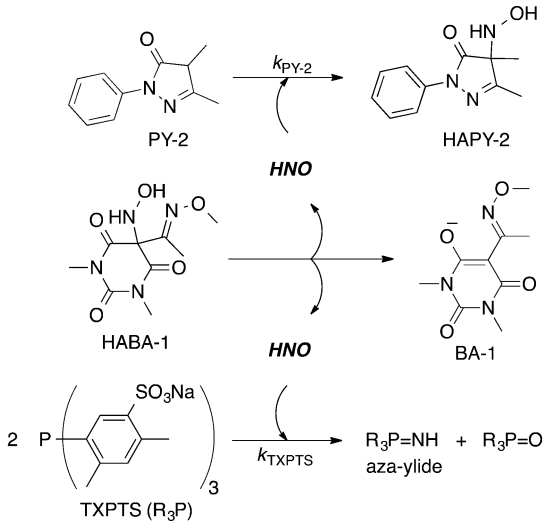

equiv of TXPTS to give the diagnostic aza-ylide product as well as the corresponding phosphine oxide, where the rate-limiting step is assumed to be the initial reaction between HNO and the first equivalent of TXPTS.

To determine the rate constant for the reaction of PY-2 with HNO (eq 1), we evaluated the concentration of TXPTS required to achieve equal product distributions of HAPY-2 compared to the aza-ylide product of TXPTS reaction.[41,42] Importantly, all the HNO produced under these conditions must react with either PY-2 or TXPTS in order for eq 1 to be valid; HNO dimerization cannot occur.

$$k_{PY\text{-}2} = \frac{k_{TXPTS}[TXPTS]}{[PY\text{-}2]} \quad (1)$$

Accordingly, due to its diagnostic ^{1}H NMR signals, byproduct BA-1 (Scheme 3) served as an internal reference such that all species involved could be quantified, including the aza-ylide product of TXPTS. The results shown in Figure 3 indicate that all HNO is effectively consumed by the traps and that the concentration of TXPTS required to affect equal product distributions is ca. 8.5 mM, which gives an HNO trapping rate constant for PY-2 of ca. 8 × 10^5 M^{-1} s^{-1} at pH 7.4, 37 °C, comparable to that of TXPTS.

These results indicate that PY-2 to HAPY-2 formation is efficient and can be used diagnostically as an alternative means of HNO quantification. Also, the "HNO transfer reaction" between HABA-1 and PY-2 demonstrates that HNO donors beyond Angeli's salt can be used in the HNO−aldol reaction.

Computational Studies. We modeled the thermodynamic driving forces for three possible reactions involving HNO with the synthesized pyrazolone examples (Scheme 4). All calculations were performed with Spartan '14 at the B3LYP/6-31G* level with an SM8 solvation model for aqueous solvation.[43] Optimized geometries and vibrational frequencies were calculated for each reactant and product independently (Supporting Information). Reaction II was balanced using a hydronium cation and a water molecule on the left and right

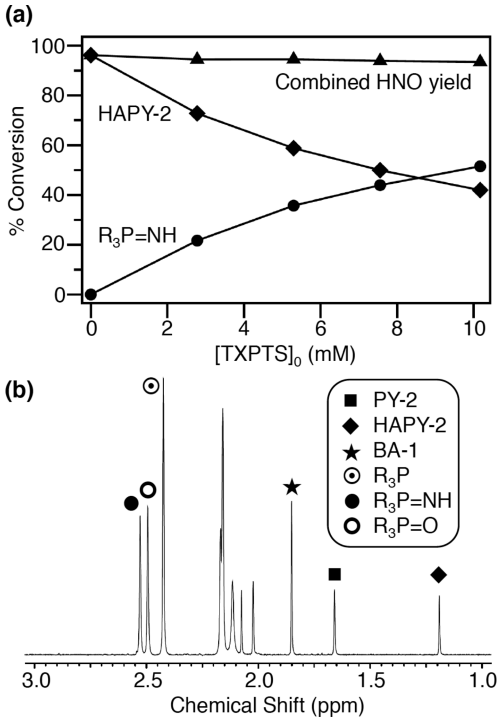

Figure 3. Competition for HABA-1-derived HNO at pH 7.4, 37 °C: PY-2 vs TXPTS. (a) All competition reactions contained HABA-1 (5 mM) and PY-2 (5 mM) in 2.0 mL of 10% D_2O, pH 7.4 phosphate buffer (0.25 M) with DTPA (0.2 mM). Each reaction was incubated under argon for 30 min at 37 °C to ensure complete decomposition of HABA-1 before ^{1}H NMR analysis of the reaction mixture. (b) Representative ^{1}H NMR spectrum of the reaction mixture, and each designated signal was used in the postreaction analysis.

Scheme 4. Possible Reactions Involving HNO with Pyrazolones[a]

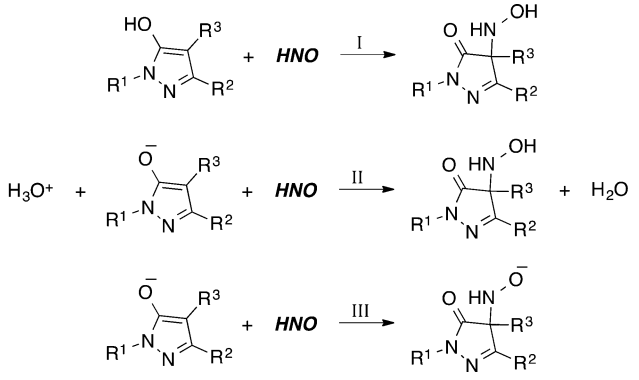

[a]Reactions: (I) HNO with neutral PY in the enol tautomer to give neutral HAPY, (II) HNO with the enolate of PY to give neutral HAPY, and (III) HNO with the enolate of PY to give HAPY oxyanion.

side of the reaction, respectively. Table 2 shows the Gibbs free energy differences for reactions I−III.

Consistent with the experimental results above, these calculations indicate that both reaction I and, particularly, reaction II are thermodynamically favorable for the forward PY plus HNO to HAPY reaction for all examples. On the other hand, reaction III is thermodynamically unfavorable, indicating that HNO formation is dependent on HAPY oxyanion formation. In addition, ground-state structures were not found for the oxyanions of HAPY-1, HAPY-3, HAPY-5, and

DOI: 10.1021/jo502330w
J. Org. Chem. 2015, 80, 1338−1348

Table 2. Gibbs Free Energy Differences in Reactions I–III

entry	R^1	R^2	R^3	ΔG_I° (kcal/mol)	ΔG_{II}° (kcal/mol)	ΔG_{III}° (kcal/mol)
1	Ph	Me	C(=NOMe)Me	−0.7	−27.5	*a*
2	Ph	Me	Me	−13.0	−34.4	13.7
3	Me	Me	C(=NOMe)Me	−0.6	−30.6	*a*
4	Me	Me	Me	−13.1	−38.7	10.2
5	H	Me	C(=NOMe)Me	−0.6	−30.8	*a*
6	H	Me	Me	−12.5	−38.1	10.9
7	4-ClPh	Me	Me	−13.0	−33.5	14.0
8	2-ClPh	Me	Me	−12.2	−36.3	12.0
9	Me	Ph	Me	−10.8	−34.7	13.2
10	Ph	Ph	Me	−11.0	−31.5	*a*
11	Me	4-ClPh	Me	−10.6	−34.3	14.6
12	Me	2-ClPh	Me	−8.0	−32.8	15.8

[a]Ground-state structures were not found for these oxyanions since the calculated structures resemble dissociated HNO and the corresponding organic byproduct. Free energies are given for 298.15 K.

HAPY-10 since the calculated structures resemble dissociated HNO and the corresponding PY byproduct. Thus, HNO generation from the expanded HAPY class is expected to be dependent on the pK_a of the HAPY donor, which in turn is likely dependent on the pK_a of the PY bydroduct.

HNO Release from the Expanded HAPY Class. As described above, the reaction of HNO with pyrazolones can be taken advantage of synthetically and potentially used as an alternative means of quantifying HNO production. However, the original purpose of this investigation was to study the HNO production *from* these newly prepared HAPY compounds. With this reversible reactivity in mind, an additional trap for HNO is required to drive the HAPY to PY reaction forward. We had demonstrated this earlier by using GSH, a biologically relevant trap for HNO in vivo. However, TXPTS is best suited for these mechanistic studies since it has selective and irreversible reactivity with HNO, and the diagnostic aza-ylide singlet in the ^{1}H NMR spectrum is distinct from the HAPY and PY compounds.

We first examined the effect that increasing [TXPTS] has on the half-life of HAPY-2, as an example. Following a 48 h incubation of HAPY-2 with 0–20 equiv of TXPTS in pH 7.4 phosphate buffer at 37 °C, ^{1}H NMR analysis indicates the incremental consumption of HAPY-2 with TXPTS increasing from 0 to ca. 4 equiv, whereas the relative percentage of HAPY-2 remains effectively unchanged when TXPTS exceeded ca. 4 equiv (Figure 4). These results highlight the reversibility of HNO generation from the HAPY series as the equilibrium favors HAPY-2 formation at low (0–4 equiv) [TXPTS], while HNO generation is rendered irreversible at high (>4 equiv) [TXPTS]. Conversely, the reaction of HNO with TXPTS (or biologically relevant GSH, for example) is irreversible. Importantly, these results also indicate no bimolecular, direct reaction between TXPTS and HAPY-2, since HAPY-2 consumption is not linear with the change in initial [TXPTS].

The timecourse for the disappearance of HAPY-2 and appearance of PY-2 and HNO (trapped as the TXPTS aza-ylide) with ca. 6 equiv of TXPTS as well as representative ^{1}H NMR spectra at t = 0, 240, and 480 h are shown in Figure 5. With a half-life of 47 h and a quantitative TXPTS aza-ylide yield, HAPY-2 is a very long-lived, yet pure, HNO donor.

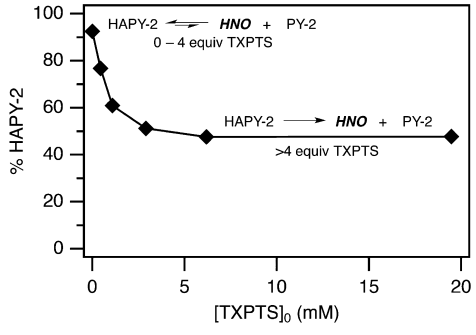

Figure 4. Incubation of HAPY-2 at pH 7.4, 37 °C after 48 h as a function of $[TXPTS]_0$. Conditions: HAPY-2 (1 mM) in 10% D_2O, pH 7.4 phosphate buffer (0.25 M) with DTPA (0.2 mM) at 37 °C under argon.

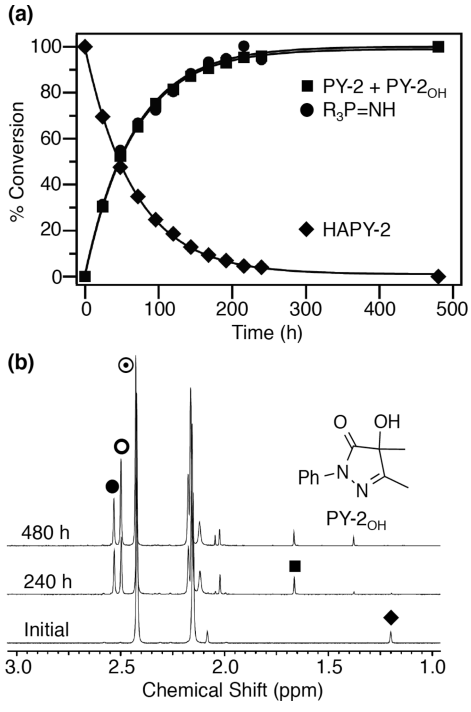

Figure 5. (a) Timecourse for the disappearance of HAPY-2 and appearance of PY-2 and TXPTS aza-ylide with added TXPTS (6 equiv). The solid curves are calculated best fits to a single exponential function ($k = 4.1 \times 10^{-6}$ s^{-1} for each fit). (b) ^{1}H NMR spectra at t = 0, 240, and 480 h; see the Experimental Section for details.

DOI: 10.1021/jo502330w
J. Org. Chem. 2015, 80, 1338–1348

Table 3. Incubation of HAPY-1−HAPY-12 in pH 7.4 Phosphate Buffer at 37 °C under Argon with Added TXPTS

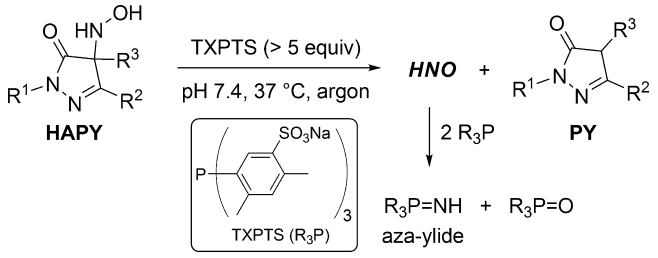

HAPY[a]	R^1	R^2	R^3	$t_{1/2}$ (min)	k (s^{-1})[b]	PY pK_a[c]
1	Ph	Me	C(=NOMe)Me	4	3.0×10^{-3}	6.0 (6.8)
2	Ph	Me	Me	2793	4.1×10^{-6}	7.6 (8.8)
3	Me	Me	C(=NOMe)Me	11	1.0×10^{-3}	6.7 (7.4)
4	Me	Me	Me	5674	2.0×10^{-6}	8.5 (9.5)
5	H	Me	C(=NOMe)Me	14	8.2×10^{-4}	7.3 (8.2)
6	H	Me	Me	4585	2.5×10^{-6}	9.0 (10.0)
7	4-ClPh	Me	Me	1473	7.8×10^{-6}	(8.4)
8	2-ClPh	Me	Me	1887	6.1×10^{-6}	7.6 (8.7)
9	Me	Ph	Me	753	1.5×10^{-5}	7.6 (8.5)
10	Ph	Ph	Me	460	2.5×10^{-5}	(8.1)
11	Me	4-ClPh	Me	799	1.4×10^{-5}	(8.0)
12	Me	2-ClPh	Me	71	1.6×10^{-4}	(8.0)

[a]Incubation conditions: HAPY (1 mM) and TXPTS (5 mM) in 10% D_2O, pH 7.4 phosphate buffer (0.25 M) with DTPA (0.2 mM) at 37 °C under argon. HNO yields are quantitative for all examples. [b]The rates are calculated best fits to a single exponential function of the integrated ^{1}H NMR data for HAPY disappearance/PY appearance. [c]The pK_a values were determined by titration in water; the values in parentheses were determined in 50% v/v aqueous ethanol.

Fortunately, under these anaerobic assay conditions, the TXPTS aza-ylide product is stable. The TXPTS oxide product slowly increases beyond the expected stoichiometric amount due to oxidation of the excess TXPTS (Figure 5b), as maintaining a rigorously anaerobic assay condition for this extended time period is experimentally challenging.

Likewise, an unknown oxidation product forms slowly from the organic byproduct PY-2 (Figure 5). Following overnight aerobic incubation of PY-2 alone in pH 7.4 phosphate buffer at 37 °C in the absence of metal chelator, the oxidized product precipitated from solution, which was briefly reheated to affect recrystallization. Single-crystal X-ray crystallography confirmed the identity of the oxidized product as PY-2_{OH}, the corresponding alcohol of PY-2 (Supporting Information). Recall that PY-2 is a derivative of edaravone, which has beneficial effects attributed to its free radical scavenging ability through a single electron transfer mechanism with reactive oxygen species such as hydroxyl and peroxyl radicals.[44] Also, the relatively rapid aerobic oxidation of PY-2 alone versus PY-2_{OH} formation under the conditions outlined in Figure 5 suggests that PY-2 is effectively inert to oxidation via the TXPTS oxide product (R_3P=O). Therefore, this ^{1}H NMR assay for the evaluation of half-life and HNO production requires the use of excess TXPTS (>5 equiv) under anaerobic conditions in order to reduce complications from the reverse reaction, PY plus HNO to give HAPY, as well as from TXPTS and PY oxidation.

The half-life of HAPY-1 was previously reported to be 9.5 min in pH 7.4 phosphate buffer at 37 °C, which was determined by UV−vis analysis in the absence of an additional trap for HNO (such as TXPTS).[27] Following the ^{1}H NMR assay described above, the observed half-life of HAPY-1 is reduced in half to 4 min, presumably due to minimization of the reverse reaction, PY-1 plus HNO to give HAPY-1 (Table 3).

Next, we explored the perhaps more subtle effects at the R^1 and R^2 positions with additional examples, specifically HAPY-3−HAPY-12. With a variety of derivatives in hand, we followed their decomposition according to the ^{1}H NMR protocol used for HAPY-1 and HAPY-2 described above. We also measured the pK_a values of their respective PY byproducts by titration in water (solubility permitting). For comparison, the pK_a values of all PY examples were also determined in 50% v/v aqueous ethanol. The results are shown in Table 3.

First, we changed the R^1 position from phenyl in HAPY-1 and HAPY-2 to methyl (HAPY-3 and HAPY-4, respectively) and hydrogen (HAPY-5 and HAPY-6, respectively). As the R^1 substituent is changed from phenyl to methyl or hydrogen, we observe a decrease in dissociation rate, which seems to correlate well with the pK_a values of the respective PY byproducts. Although the R^3 = *O*-methyloxime derivatives, HAPY-3 and HAPY-5, have half-lives between those of HAPY-1 and HAPY-2, the R^3 = methyl derivatives, HAPY-4 and HAPY-6, have even slower dissociation rates than HAPY-2. Importantly, the HNO yield for all of these precursors remains quantitative, and as such, HAPY-4 and HAPY-6 are the longest lived reported pure HNO donors to date with half-lives measuring 95 and 76 h, respectively.

Next, we explored substitution on the phenyl ring of HAPY-2 with 4-chloro (HAPY-7) and 2-chloro (HAPY-8) groups. These derivatives have slightly faster rates when compared to HAPY-2 but are still over 2 orders of magnitude slower than HAPY-1.

We then made changes to the R^2 position first by synthesizing HAPY-9, the isomer of HAPY-2. Interestingly, the decomposition rate of HAPY-9 is over three times faster than that of HAPY-2. The impact of R^2 substitution is best

DOI: 10.1021/jo502330w
J. Org. Chem. 2015, 80, 1338−1348

illustrated by comparing HAPY-4 with HAPY-9, HAPY-11, and HAPY-12, where the observed rate changes span 2 orders of magnitude.

All told, by varying groups at the R^1, R^2, and R^3 positions on the pyrazolone ring, the observed rate changes span 1, 2, and 3 orders of magnitude, respectively. The distance removed from the PY's 3-position carbon, formerly bearing the hydroxylamine, is greatest for the R^1 position and shortest for the R^3 position, and inductive effects are expected to follow likewise. However, only the R^3 position allows for additional resonance stabilization in the dissociated PY byproduct. Because of the combined resonance and inductive stabilization effects, the impact on the PY byproduct pK_a is greatest when the R^3 position is varied. Given the relatively large pK_a difference of two units for PY-1 and PY-2, this must be a contributing factor in the large difference in decomposition rates of the corresponding HAPY products (Table 3).

As suggested from our calculations, HNO release is governed by the HAPY pK_a, which likely correlates with the PY pK_a. This correlation is confirmed by the UV–vis–determined decomposition rates for HAPY-1 and HAPY-2 as a function of pH, where the observed sharp increases reflect rapid PY formation presumably as a result of HAPY deprotonation (Figure 6a).

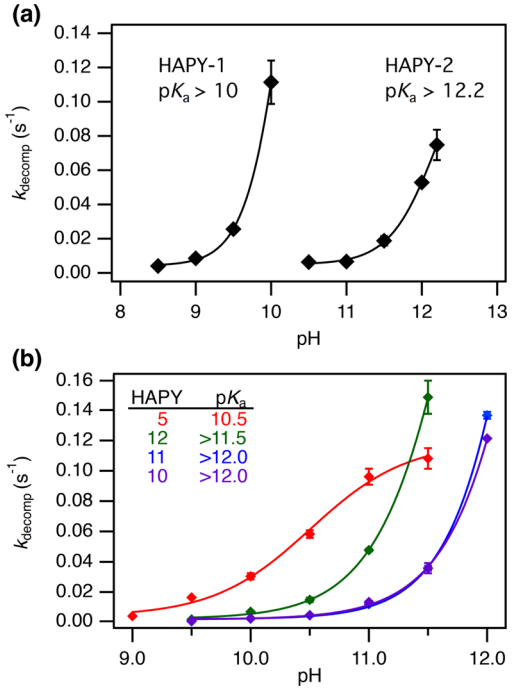

Figure 6. Plot of UV–vis determined decomposition rates as a function of pH in 0.1 M phosphate buffer at 25 °C (SEM ± 10%; $n \geq 3$) for (a) HAPY-1 and HAPY-2, and (b) HAPY-5 (red), HAPY-12 (green), HAPY-11 (blue), and HAPY-10 (purple). For HAPY-5, the solid curve is a calculated best fit to a sigmoid function (pK_a = 10.5).

Decomposition rates reach the time resolution limit (ca. 0.15 s^{-1}) of the UV–vis experiment, precluding a complete pK_a analysis for each donor as the magnitude of the sigmoidal curve extends well beyond experimental parameters. However, these results suggest that (1) the pK_a difference of HAPY-1 and HAPY-2 is also ca. two units, corresponding well to the PY-1/PY-2 pK_a difference, (2) the observed sharp increases in k values as a function of pH is not likely related to HNO deprotonation (pK_a ~11.4) since this behavior is observed with HAPY-1 (pK_a > 10) and HABA-1 (pK_a > 9),[27] and (3) the barrier to dissociation must be very low once HAPY deprotonation occurs. Moreover, with such large approximate pK_a values, HNO evolution at neutral pH suggests a near barrierless dissociation from the deprotonated donor.

However, the PY pK_a alone does not always correlate with the HAPY pK_a. For example, the pK_a values of PY-5, PY-10 – PY-12 are all ca. 8 in 50% v/v aqueous ethanol (Table 3), yet HAPY-5 (pK_a = 10.5) is more acidic than HAPY-12 (pK_a > 11.5), which in turn is more acidic than HAPY-10 and HAPY-11 (pK_a > 12.0) (Figure 6b). This trend is mirrored in the half-lives of these HAPY examples at neutral pH (Table 3); the half-lives of HAPY-5, HAPY-10, HAPY-11, and HAPY-12 are 14, 460, 799, and 71 min, respectively. These results suggest that the HAPY pK_a, as opposed to the PY pK_a, is a better predictor of HNO generation rate under physiological conditions. The fact that decomposition of HAPY-5 as a function of pH approaches a limiting rate constant at a pH apparently much lower than that for HAPY-10–HAPY-12 in this analysis (Figure 6b), suggests contribution from deprotonation at the R^1 position proton (*N*-H) of the pyrazolone ring (Scheme 5).

Scheme 5. Proposed Mechanism of HNO Release

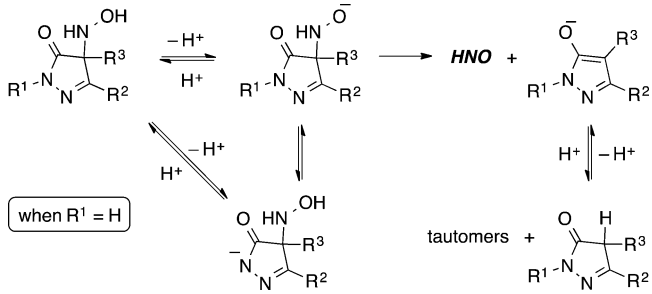

This may explain the greater acidity of HAPY-5. In comparison, a pK_a value of 11.5 is estimated for the R^1 position proton of HAPY-6, the R^3 = methyl analog of HAPY-5 (Supporting Information). For the HAPY class as a whole, HNO release following *H*OHN-PY deprotonation remains the most plausible mechanism in water (Scheme 5).

The pK_a values of the PY byproducts are a reflection of the weighted average of the various tautomers that are known to exist in pyrazolones, such as edaravone.[45–47] Presumably, the pK_a value related to deprotonation of the PY's 3-position carbon, formerly bearing the hydroxylamine, is the most relevant to predicting SAR for HNO release; however, we can assume from this first HAPY series extension study that PY byproducts with measured pK_a values ≤ ca. 8 in 50% v/v aqueous ethanol are useful targets for further development of the HAPY class of HNO donors.

■ CONCLUSION

HNO has been shown to enhance myocardial function, demonstrating its potential usefulness in the treatment of heart failure. The HAPY class of HNO donors represents a new and robust platform capable of producing HNO quantitatively over extended periods of time along with a PY byproduct that is related to edaravone, a potent antioxidant already in clinical use for the treatment of stroke and cardiovascular disease. The HNO release rate is highly tunable by varying the groups at the R^1, R^2, and R^3 positions on the pyrazolone ring; the effect of the R-position on half-life is $R^3 > R^2 > R^1$. Experimental and

DOI: 10.1021/jo502330w
J. Org. Chem. 2015, 80, 1338–1348

computational investigations suggest that the HNO release rate correlates with the HAPY and PY pK_a values. The catch is a strong affinity that is shared between HNO and the released PY byproduct since the bimolecular rate constant in pH 7.4 phosphate buffer at 37 °C can reach 8×10^5 M^{-1} s^{-1}. Given that biological targets for HNO are in excess of HNO in vivo, the reverse reaction of PY plus HNO to give HAPY is expected to be negligible under these conditions; thus, we believe these donors will be useful in in vivo studies. This is also the case in the reported ^{1}H NMR assay for the evaluation of half-life and HNO production utilizing the selective, distinctive, and irreversible trap for HNO, TXPTS. Yet, this reverse reaction, described herein for the first time as the HNO-aldol reaction with pyrazolones, is an efficient, alternative synthetic strategy to the cumbersome, three-step bromination-displacement-deprotection strategy, thus illustrating a synthetically useful route to HAPY donors. We anticipate utilizing these methodologies for the development of new *N*-substituted hydroxylamines with other suitable carbon-based leaving groups.

EXPERIMENTAL SECTION

Materials. All starting materials were of reagent grade and used without further purification. Angeli's salt ($Na_2N_2O_3$);[48] compounds PY-1 and HAPY-1;[27] PY-2, PY-4, PY-9, and PY-10;[49] PY-6;[50] PY-11 and *N*-methyl-3-(2-chlorophenyl)pyrazolone;[51] and 4-acetyl-3-methylpyrazolone[52] are all known compounds and were prepared according to literature procedures. Tris(4,6-dimethyl-3-sulfanatophenyl)-phosphine trisodium salt (TXPTS) was of reagent grade and used without further purification. Synthetic TXPTS aza-ylide was obtained through the amidation of TXPTS using hydroxylamine *O*-sulfonic acid in water.[53] Melting point measurements are uncorrected. NMR spectra were obtained on a 400 MHz FT-NMR spectrometer. All chemical shifts are reported in parts per million (ppm) relative to residual $CHCl_3$ (7.26 ppm for ^{1}H, 77.2 ppm for ^{13}C), residual DMSO (2.50 ppm for ^{1}H, 39.5 for ^{13}C), or residual MeOH (3.31 ppm for ^{1}H, 49.2 ppm for ^{13}C). High-resolution mass spectra were obtained on a magnetic sector mass spectrometer operating in fast atom bombardment (FAB) mode. Ultraviolet-visible (UV-vis) absorption spectra were obtained using a diode array spectrometer. Buffered solutions (0.1 M) for UV-vis experiments were prepared from Na_2PO_3H/Na_3PO_4 (pH 8.5, 9.0, 9.5, 10.0, 10.5, 11.0, 11.5, 12.0, 12.2).

^{1}H NMR Incubation Procedure of HAPY Donors at pH 7.4, 37 °C with TXPTS. *General Methods.* All ^{1}H NMR spectra were obtained in pH 7.4 solution containing 0.25 M phosphate buffer, 0.2 mM of the metal chelator diethylenetriaminepentaacetic acid (DTPA), and 10% D_2O on a 400 MHz FT-NMR spectrometer using a 1 s presaturation pulse to suppress the water signal. Each free induction decay was Fourier transformed, phased, and baseline-corrected, and integral areas were measured for the methyl groups of compounds HAPY-1–HAPY-12 and PY-1–PY-2 and the downfield methyl group of TXPTS aza-ylide. The ^{1}H NMR spectrum of the HNO-derived TXPTS aza-ylide product matched that of synthetic TXPTS aza-ylide. The HNO yield from compounds HAPY-1–HAPY-12 was determined from the final TXPTS aza-ylide yield.

Procedure. The ^{1}H NMR procedure used was based on an HPLC protocol developed by King and co-workers.[40,41] To an argon-purged NMR solution (1.00 mL) containing TXPTS (3.3 mg, 5 mM) was added HAPY (10 μL of 100 mM in methanol-d_4) to give 1 mM as the initial concentration of HAPY. The solution was briefly mixed, ca. 0.5 mL was transferred to an argon-purged NMR tube, and an initial ^{1}H NMR spectrum was obtained. The sample was then either (1) externally incubated at 37 °C and ^{1}H NMR spectra were collected at regular time intervals or (2) internally incubated at 37 °C and ^{1}H NMR spectra were collected using a canned pulse sequence, zg2d, modified to include a 1 s presaturation pulse during the relaxation delay.

General HNO–Aldol Procedure. To the PY substrate (0.20 mmol), Angeli's salt (49 mg, 0.40 mmol), and powdered DTPA (39 mg, 0.10 mmol) under argon at room temperature was added a degassed mixture of 50% v/v aqueous ethanol (1 mL) via syringe. The reaction was allowed to stir for 1.5 h, diluted with ethanol (>5 mL), and concentrated to dryness in vacuo with minimum heat (<30 °C). The material was then taken up in minimum ethanol, eluted through a short silica plug, and concentrated in vacuo to give the desired HAPY product or to allow for further purification if complete conversion was not observed (i.e., for the *O*-methyloxime derivatives HAPY-1, HAPY-3, and HAPY-5). The crude reaction mixture was loaded with methanol onto an analytical TLC plate (250 μm thickness) and developed in either 50% v/v ethyl acetate/dichloromethane (HAPY-1) or ethyl acetate (HAPY-3 and HAPY-5). The product band (R_f > 0.5) was scraped off the plate into a flask using a metal spatula. The product was eluted with methanol (10 mL), filtered through cotton, and concentrated in vacuo to yield the desired HAPY product typically as off-white/white solids. Isolated yields are given in Table 1.

4-(N-Hydroxylamino)-4-methyl-N-phenyl-3-methylpyrazolone (HAPY-2). Mp: 152–154 °C. ^{1}H NMR (400 MHz, $CDCl_3$) δ: 7.93 (d, 2H, *J* = 8.8 Hz), 7.40 (dd, 2H, *J* = 7.4 Hz), 7.18 (t, 1H, *J* = 7.4 Hz), 5.70 (bs, 1H), 4.77 (s, 1H), 2.21 (s, 3H), 1.28 (s, 3H). ^{13}C NMR (100 MHz, $CDCl_3$) δ: 174.1, 162.1, 138.1, 129.1, 125.3, 118.9, 71.2, 17.0, 13.3. HR-MS (FAB): found *m*/*z* = 220.10932 (MH^+), calcd for $C_{11}H_{14}N_3O_2$ 220.10860 (MH^+).

4-(N-Hydroxylamino)-4-(acetyl-O-methoxyoxime)-N-methyl-3-methylpyrazolone (HAPY-3). Mp: 105–108 °C. ^{1}H NMR (400 MHz, $CDCl_3$) δ: 6.12 (s, 1H), 4.67 (s, 1H), 3.90 (s, 3H), 3.33 (s, 3H), 2.12 (s, 3H), 1.74 (s, 3H). ^{13}C NMR (100 MHz, $CDCl_3$) δ: 171.7, 159.0, 76.6, 62.5, 31.8, 14.4, 11.0. HR-MS (FAB): found *m*/*z* = 215.11454 (MH^+), calcd for $C_8H_{15}N_4O_3$ 215.11442 (MH^+).

4-(N-Hydroxylamino)-4-methyl-N-methyl-3-methylpyrazolone (HAPY-4). Mp: 135–137 °C. ^{1}H NMR (400 MHz, DMSO-d_6) δ: 7.52 (d, 1H, *J* = 2.8 Hz), 6.25 (d, 1H, *J* = 2.8 Hz), 3.12 (s, 3H), 1.96 (s, 3H), 1.00 (s, 3H). ^{13}C NMR (100 MHz, DMSO-d_6) δ: 175.3, 161.9, 69.0, 30.7, 16.0, 12.7. HR-MS (FAB): found *m*/*z* = 158.09320 (MH^+), calcd for $C_6H_{12}N_3O_2$ 158.09295 (MH^+).

4-(N-Hydroxylamino)-4-(acetyl-O-methoxyoxime)-3-methylpyrazolone (HAPY-5). Mp: 148–150 °C. ^{1}H NMR (400 MHz, DMSO-d_6) δ: 10.96 (s, 1H), 7.76, (d, 1H, *J* = 2.7 Hz), 6.60 (d, 1H, *J* = 2.7 Hz), 3.76 (s, 3H), 1.98 (s, 3H), 1.79 (s, 3H). ^{13}C NMR (100 MHz, DMSO-d_6) δ: 173.9, 159.5, 151.8, 74.2, 61.6, 14.9, 10.6. HR-MS (FAB): found *m*/*z* = 201.09920 (MH^+), calcd for $C_7H_{13}N_4O_3$ 201.09817 (MH^+).

4-(N-Hydroxylamino)-4-methyl-3-methylpyrazolone (HAPY-6). Mp: 185–187 °C. ^{1}H NMR (400 MHz, DMSO-d_6) δ: 10.77 (s, 1H), 7.50 (d, 1H, *J* = 2.9 Hz), 6.16 (d, 1H, *J* = 2.9 Hz), 1.93 (s, 3H), 0.97 (s, 3H). ^{13}C NMR (100 MHz, DMSO-d_6) δ: 178.3, 161.9, 68.0, 16.0, 13.0. HR-MS (FAB): found *m*/*z* = 144.07683 (MH^+), calcd for $C_5H_{10}N_3O_2$ 144.07730 (MH^+)..

4-(N-Hydroxylamino)-4-methyl-N-(4-chlorophenyl)-3-methylpyrazolone (HAPY-7). Mp: 157–159 °C. ^{1}H NMR (400 MHz, $CDCl_3$) δ: 7.90 (d, 2H, *J* = 9.0 Hz), 7.35 (d, 2H, *J* = 9.0 Hz), 5.66 (d, 1H, *J* = 2.8 Hz), 4.45 (d, 1H, *J* = 2.8 Hz), 2.20 (s, 3H), 1.28 (s, 3H). ^{13}C NMR (100 MHz, $CDCl_3$) δ: 174.0, 162.2, 136.8, 130.4, 129.1, 119.9, 71.2, 16.9, 13.3. HR-MS (FAB): found *m*/*z* = 254.06968 (MH^+,^{35}Cl), 256.06703 (MH^+,^{37}Cl), calcd for $C_{11}H_{13}ClN_3O_2$ 254.06963 (MH^+,^{35}Cl), 256.06668 (MH^+,^{37}Cl).

4-(N-Hydroxylamino)-4-methyl-N-(2-chlorophenyl)-3-methylpyrazolone (HAPY-8). Mp: 150–152 °C. ^{1}H NMR (400 MHz, DMSO-d_6) δ: 7.73 (d, 1H, *J* = 2.8 Hz), 7.60 (m, 1H), 7.43 (m, 3H), 6.50 (d, 1H, *J* = 2.8 Hz), 2.07 (s, 3H), 1.17 (s, 3H). ^{13}C NMR (100 MHz, DMSO-d_6) δ: 174.8, 163.3, 134.8, 130.8, 130.1, 129.9, 129.1, 128.0, 69.4, 16.2, 12.9. HR-MS (FAB): found *m*/*z* = 254.06967 (MH^+,^{35}Cl), 256.06718 (MH^+,^{37}Cl), calcd for $C_{11}H_{13}ClN_3O_2$ 254.06963 (MH^+,^{35}Cl), 256.06668 (MH^+,^{37}Cl).

4-(N-Hydroxylamino)-4-methyl-N-methyl-3-phenylpyrazolone (HAPY-9). Mp: 146–148 °C. ^{1}H NMR (400 MHz, DMSO-d_6) δ: 8.06 (m, 2H), 7.64 (d, 2H, *J* = 2.5 Hz), 7.45 (m, 3H), 6.48 (d, 2H, *J* = 2.5 Hz), 3.29 (s, 3H), 1.21 (s, 3H). ^{13}C NMR (100 MHz, DMSO-d_6) δ: 176.1, 157.4, 130.4, 129.9, 128.6, 126.2, 69.3, 31.2, 17.9. HR-MS

DOI: 10.1021/jo502330w
J. Org. Chem. 2015, 80, 1338–1348

(FAB): found m/z = 220.10897 (MH^+), calcd for $C_{11}H_{14}N_3O_2$ 220.10860 (MH^+).

4-(N-Hydroxylamino)-4-methyl-N-phenyl-3-phenylpyrazolone (HAPY-10). Mp: 148−150 °C. ^{1}H NMR (400 MHz, $CDCl_3$) δ: 8.21 (m, 2H), 8.05 (m, 2H), 7.45 (m, 5H), 7.24 (m, 1H), 5.95 (d, 1H, J = 3.2 Hz), 4.50 (d, 1H, J = 3.3 Hz), 1.48 (s, 3H). ^{13}C NMR (100 MHz, $CDCl_3$) δ: 175.0, 157.7, 138.2, 131.0, 130.3, 129.1, 129.1, 126.8, 125.5, 119.0, 71.5, 18.9. HR-MS (FAB): found m/z = 282.12461 (MH^+), calcd for $C_{16}H_{16}N_3O_2$ 282.12425 (MH^+).

4-(N-Hydroxylamino)-4-methyl-N-methyl-3-(4-chlorophenyl)-pyrazolone (HAPY-11). Mp: 182−184 °C. ^{1}H NMR (400 MHz, DMSO-d_6) δ: 8.06 (d, 2H, J = 8.7 Hz), 7.66 (d, 1H, J = 2.6 Hz), 7.53 (d, 2H, J = 8.7 Hz), 6.54 (d, 1H, J = 2.6 Hz), 3.29 (s, 3H), 1.19 (s, 3H). ^{13}C NMR (100 MHz, DMSO-d_6) δ: 176.1, 156.4, 134.5, 129.2, 128.7, 128.0, 62.3, 31.2, 17.7. HR-MS (FAB): found m/z = 254.06941 (MH^+, ^{35}Cl), 256.06193 (MH^+, ^{37}Cl), calcd for $C_{11}H_{13}ClN_3O_2$: 254.06963 (MH^+, ^{35}Cl), 256.06668 (MH^+, ^{37}Cl).

4-(N-Hydroxylamino)-4-methyl-N-methyl-3-(2-chlorophenyl)-pyrazolone (HAPY-12). Mp: 126−128 °C. ^{1}H NMR (400 MHz, $CDCl_3$) δ: 7.71 (m, 1H), 7.50 (m, 1H), 7.38 (m, 2H), 5.90 (br, 2H), 3.45 (s, 3H), 1.26 (s, 3H). ^{13}C NMR (100 MHz, $CDCl_3$) δ: 174.9, 158.6, 133.5, 131.1, 131.1, 130.7, 129.3, 127.1, 71.6, 32.0, 16.9. HR-MS (FAB): found m/z = 254.06981(MH^+, ^{35}Cl), 256.06755 (MH^+, ^{37}Cl), calcd for $C_{11}H_{13}ClN_3O_2$ 254.06963 (MH^+, ^{35}Cl), 256.06668 (MH^+, ^{37}Cl).

4-Acetyl-1,3-dimethylpyrazolone (1). To methyl acetoacetate (2.32 g, 20 mmol) on ice was added methylhydrazine (1.05 mL, 20 mmol) over 2−3 min with stirring. The reaction was then stirred for 5 min, whereupon 1,3-dimethylpyrazolone precipitated from solution. The reaction was diluted with ethanol (20 mL) and concentrated in vacuo to give dry 1,3-dimethylpyrazolone as an off-white solid. This was then taken up with trimethyl orthoacetate (10 mL) under nitrogen and heated to 65 °C for 2 h. The clear, red-orange solution was concentrated in vacuo, the solid was dissolved in water (10 mL), and the solution was allowed to stand at 4 °C overnight. Filtration of the resulting precipitate gave the title compound as an orange solid (1.36 g, 44%). Mp: 118−120 °C. ^{1}H NMR (400 MHz, $CDCl_3$) δ: 3.55 (s, 3H), 2.38 (s, 3H), 2.36 (s, 3H). ^{13}C NMR (100 MHz, $CDCl_3$) δ: 195.3, 159.6, 146.8, 103.2, 32.5, 27.5, 15.5. HR-MS (FAB): found m/z = 155.08184 (MH^+), calcd for $C_7H_{11}N_2O_2$ 155.08205 (MH^+).

3-(2-Chlorophenyl)-4-formyl-1-methylpyrazolone (2). To ethyl (2-chlorobenzoyl)acetate (0.937 g, 4.13 mmol) at room temperature was added methylhydrazine (0.22 mL, 4.1 mmol) over two to 3 min with stirring. The reaction was then heated to 90 °C for 15 min and allowed to cool to room temperature where white solids formed upon standing. This material was recrystallized from hot ethanol and water to give pure *N*-methyl-3-(2-chlorophenyl)-pyrazolone (0.410 g, 48%). To this product dissolved in dimethylformamide (1 mL) was added phosphoryl chloride (0.13 mL, 1.4 mmol), and the reaction was heated to 65 °C with stirring for 2 h followed by addition of water (5 mL). This solution was allowed to stand at room temperature for 1 d, and the resultant yellow precipitate was collected by vacuum filtration to give the title compound (0.370 g, 79%). Mp: 163−165 °C. ^{1}H NMR (400 MHz, DMSO-d_6) δ: 9.51 (s, 1H), 7.44 (m, 4H), 3.60 (s, 3H). ^{13}C NMR (100 MHz, DMSO-d_6) δ: 182.0, 155.6, 132.9, 132.2, 131.7, 130.2, 129.3, 126.9, 104.4, 33.1. HR-MS (FAB): found m/z = 237.04354 (MH^+,^{35}Cl), 239.04114 (MH^+,^{37}Cl); calcd for $C_{11}H_{10}ClN_2O_2$: 237.04308 (MH^+,^{35}Cl), 239.04013 (MH^+,^{37}Cl).

4-(Acetyl-O-methoxyoxime)-1,3-dimethylpyrazolone (PY-3). Compound **1** (0.771 g, 5 mmol), *O*-methylhydroxylamine hydrochloride (0.459 g, 5.5 mmol), and sodium bicarbonate (0.462 g, 5.5 mmol) were taken up in methanol (50 mL), and the reaction was refluxed with stirring for 2 h followed by concentration in vacuo. The resultant material was taken up in dichloromethane, filtered through cotton, and concentrated in vacuo to give the title compound as an off-white solid (0.731 g, 80%). Mp: 105−107 °C. ^{1}H NMR (400 MHz, $CDCl_3$) δ: 3.85 (s, 3H), 3.56 (s, 3H), 2.29 (s, 3H), 2.19 (s, 3H). ^{13}C NMR (100 MHz, $CDCl_3$) δ: 155.2, 153.8, 144.7, 95.2, 62.0, 32.8, 15.6, 13.1. HR-MS (FAB): found m/z = 184.10819 (MH^+), calcd for $C_8H_{14}N_3O_2$ 184.10860 (MH^+).

4-(Acetyl-O-methoxyoxime)-3-methylpyrazolone (PY-5). 4-Acetyl-3-methylpyrazolone (2.935 g, 20.9 mmol), *O*-methylhydroxylamine hydrochloride (1.921 g, 23 mmol), and sodium bicarbonate (1.932 g, 23 mmol) were taken up in methanol (125 mL), and the reaction was refluxed with stirring for 21 h followed by concentration in vacuo. The resultant material was taken up in ethyl acetated (2 × 125 mL), filtered through cotton, and concentrated in vacuo to give the title compound as a pale yellow solid (2.487 g, 70%). Mp: 189−191 °C. ^{1}H NMR (400 MHz, DMSO-d_6) δ: 3.78 (s, 3H), 2.23 (s, 3H), 2.08 (s, 3H). ^{13}C NMR (100 MHz, DMSO-d_6) δ: 159.9, 151.5, 138.2, 98.5, 61.0, 13.5, 12.2. HR-MS (FAB): found m/z = 170.09335 (MH^+), calcd for $C_7H_{12}N_3O_2$ 170.09295 (MH^+).

4-Methyl-N-(4-chlorophenyl)-3-methylpyrazolone (PY-7). Ethyl 2-methylacetoacetate (0.71 mL, 5 mmol), 4-chlorophenylhydrazine hydrochloride (0.895 g, 5 mmol), and sodium acetate (0.410 g, 5 mmol) were taken up in ethanol (50 mL), and the reaction was refluxed with stirring for 1 d followed by filtration through cotton and concentration in vacuo. The resultant material was recrystallized from hot ethanol and 1 N HCl to give the title compound as a white solid (0.867 g, 78%). Mp: 173−175 °C. ^{1}H NMR (400 MHz, DMSO-d_6) δ: 7.75 (d, 2H, J = 8.9 Hz), 7.50 (d, 2H, J = 8.9 Hz), 2.13 (s, 3H), 1.80 (s, 3H). ^{13}C NMR (100 MHz, DMSO-d_6) δ: 157.0, 147.7, 135.7, 129.7, 129.0, 122.0, 99.3, 11.3, 6.6. HR-MS (FAB): found m/z = 223.06396 (MH^+,^{35}Cl), 225.06151 (MH^+,^{37}Cl), calcd for $C_{11}H_{12}ClN_2O$: 223.06382 (MH^+,^{35}Cl), 225.06087 (MH^+,^{37}Cl).

4-Methyl-N-(2-chlorophenyl)-3-methylpyrazolone (PY-8). Ethyl 2-methylacetoacetate (0.71 mL, 5 mmol), 2-chlorophenylhydrazine hydrochloride (0.895 g, 5 mmol), and sodium acetate (0.410 g, 5 mmol) were taken up in acetic acid (50 mL), and the reaction was refluxed with stirring for 18 h followed by filtration through cotton and concentration in vacuo. The resultant material was triturated with diethyl ether to remove the colored impurities, filtered, extracted into ethyl acetate (2 × 100 mL), washed with water and brine, dried over magnesium sulfate, filtered, and concentrated in vacuo to give the title compound as an off-white solid (0.696 g, 63%). Mp: 166−168 °C. ^{1}H NMR (400 MHz, MeOD-d_4) δ: 7.58 (m, 1H), 7.45 (m, 3H), 2.17 (s, 3H), 1.85 (s, 3H). ^{13}C NMR (100 MHz, MeOD-d_4) δ: 164.8, 148.6, 135.1, 134.3, 132.1, 131.7, 131.5, 129.1. HR-MS (FAB): found m/z = 223.06348 (MH^+,^{35}Cl), 225.06092 (MH^+,^{37}Cl), calcd for $C_{11}H_{12}ClN_2O$ 223.06382 (MH^+,^{35}Cl), 225.06087 (MH^+,^{37}Cl).

4-Methyl-N-methyl-3-(2-chlorophenyl)pyrazolone (PY-12). To a solution of compound **2** (0.370 g, 1.56 mmol) in acetic acid (20 mL) was added sodium cyanoborohydride (0.211 g, 3.2 mmol), and the reaction was heated to 65 °C and stirred for 2 h. The reaction was then concentrated in vacuo, taken up in 1 N HCl, extracted into ethyl acetate (2 × 50 mL), washed with brine, dried over magnesium sulfate, filtered, and concentrated in vacuo. The resultant viscous oil was triturated with dichloromethane and hexanes and filtered to give the title compound as a white solid (0.070 g, 20%). Mp: 168−170 °C. ^{1}H NMR (400 MHz, DMSO-d_6) δ: 7.51 (d, 1H, J = 6.8 Hz), 7.38 (m, 3H), 3.57 (s, 3H), 1.76 (s, 3H). ^{13}C NMR (100 MHz, DMSO-d_6) δ: 150.5, 145.5, 133.0, 132.7, 132.1, 129.8, 129.4, 127.0, 95.7, 33.2, 7.7. HR-MS (FAB): found m/z = 225.06188 (MH^+,^{37}Cl), calcd for $C_{11}H_{12}ClN_2O$ 225.06087 (MH^+,^{37}Cl).

■ ASSOCIATED CONTENT

Ⓢ Supporting Information

Computational results including optimized geometries, energies, and vibrational frequencies and intensities; synthetic schemes; single-crystal X-ray crystallographic data; NMR spectra. This material is available free of charge via the Internet at http://pubs.acs.org.

■ AUTHOR INFORMATION

Corresponding Author

*E-mail: jtoscano@jhu.edu.

DOI: 10.1021/jo502330w
J. Org. Chem. 2015, 80, 1338−1348

Notes

The authors declare the following competing financial interest(s): J.P.T. is a cofounder and stockholder and serves on the Scientific Advisory Board of Cardioxyl Pharmaceuticals.

■ ACKNOWLEDGMENTS

We gratefully acknowledge the National Science Foundation (CHE-1213438) and Cardioxyl Pharmaceuticals for generous support of this research. We also thank the Johns Hopkins University, Department of Chemistry Facility Managers, Dr. Cathy D. Moore (NMR spectroscopy), Dr. Maxime A. Siegler (single-crystal X-ray crystallography), and Dr. I. Phil Mortimer (HR-MS) for assistance with compound identification and characterization.

■ REFERENCES

(1) Go, A. S.; Mozaffarian, D.; Roger, V. L.; Benjamin, E. J.; Berry, J. D.; Borden, W. B.; Bravata, D. M.; Dai, S.; Ford, E. S.; Fox, C. S.; Franco, S.; Fullerton, H. J.; Gillespie, C.; Hailpern, S. M.; Heit, J. A.; Howard, V. J.; Huffman, M. D.; Kissela, B. M.; Kittner, S. J.; Lackland, D. T.; Lichtman, J. H.; Lisabeth, L. D.; Magid, D.; Marcus, G. M.; Marelli, A.; Matchar, D. B.; McGuire, D. K.; Mohler, E. R.; Moy, C. S.; Mussolino, M. E.; Nichol, G.; Paynter, N. P.; Schreiner, P. J.; Sorlie, P. D.; Stein, J.; Turan, T. N.; Virani, S. S.; Wong, N. D.; Woo, D.; Turner, M. B. *Circulation* **2013**, *127*, e6−e245.

(2) McMurray, J. J.; Petrie, M. C.; Murdoch, D. R.; Davie, A. P. *Eur. Heart J.* **1998**, *19* (Suppl P), P9−16.

(3) Heidenreich, P. A.; Trogdon, J. G.; Khavjou, O. A.; Butler, J.; Dracup, K.; Ezekowitz, M. D.; Finkelstein, E. A.; Hong, Y.; Johnston, S. C.; Khera, A.; Lloyd-Jones, D. M.; Nelson, S. A.; Nichol, G.; Orenstein, D.; Wilson, P. W. F.; Woo, Y. J. *Circulation* **2011**, *123*, 933−44.

(4) Paolocci, N.; Saavedra, W. F.; Miranda, K. M.; Martignani, C.; Isoda, T.; Hare, J. M.; Espey, M. G.; Fukuto, J. M.; Feelisch, M.; Wink, D. A.; Kass, D. A. *Proc. Natl. Acad. Sci. U.S.A.* **2001**, *98*, 10463−10468.

(5) Paolocci, N.; Katori, T.; Champion, H. C.; St. John, M. E.; Miranda, K. M.; Fukuto, J. M.; Wink, D. A.; Kass, D. A. *Proc. Natl. Acad. Sci. U.S.A.* **2003**, *100*, 5537−5542.

(6) Paolocci, N.; Jackson, M. I.; Lopez, B. E.; Miranda, K.; Tocchetti, C. G.; Wink, D. A.; Hobbs, A. J.; Fukuto, J. M. *Pharmacol. Ther.* **2007**, *113*, 442−458.

(7) Tocchetti, C. G.; Wang, W.; Froehlich, J. P.; Huke, S.; Aon, M. A.; Wilson, G. M.; Di Benedetto, G.; O'Rourke, B.; Gao, W. D.; Wink, D. A.; Toscano, J. P.; Zaccolo, M.; Bers, D. M.; Valdivia, H. H.; Cheng, H.; Kass, D. A.; Paolocci, N. *Circ. Res.* **2007**, *100*, 96−104.

(8) Froehlich, J. P.; Mahaney, J. E.; Keceli, G.; Pavlos, C. M.; Goldstein, R.; Redwood, A. J.; Sumbilla, C.; Lee, D. I.; Tocchetti, C. G.; Kass, D. A.; Paolocci, N.; Toscano, J. P. *Biochemistry* **2008**, *47*, 13150−13152.

(9) Shafirovich, V.; Lymar, S. V. *Proc. Natl. Acad. Sci. U.S.A.* **2002**, *99*, 7340−7345.

(10) Hughes, M. N.; Cammack, R. *Methods Enzymol.* **1998**, *301*, 279−287.

(11) Gladwin, M. T.; Raat, N. J. H.; Shiva, S.; Dezfulian, C.; Hogg, N.; Kim-Shapiro, D. B.; Patel, R. P. *Am. J. Physiol.: Heart Circ. Physiol.* **2006**, *291*, H2026−H2035.

(12) Gladwin, M. T.; Schechter, A. N.; Kim-Shapiro, D. B.; Patel, R. P.; Hogg, N.; Shiva, S.; Cannon, R. O.; Kelm, M.; Wink, D. A.; Espey, M. G.; Oldfield, E. H.; Pluta, R. M.; Freeman, B. A.; Lancaster, J. R.; Feelisch, M.; Lundberg, J. O. *Nat. Chem. Biol.* **2005**, *1*, 308−314.

(13) Choe, C.-U.; Lewerenz, J.; Gerloff, C.; Magnus, T.; Donzelli, S. *Antioxid. Redox Signal.* **2011**, *14*, 1699−1711.

(14) Sha, X.; Isbell, T. S.; Patel, R. P.; Day, C. S.; King, S. B. *J. Am. Chem. Soc.* **2006**, *128*, 9687−9692.

(15) Shoman, M. E.; DuMond, J. F.; Isbell, T. S.; Crawford, J. H.; Brandon, A.; Honovar, J.; Vitturi, D. A.; White, C. R.; Patel, R. P.; King, S. B. *J. Med. Chem.* **2011**, *54*, 1059−1070.

(16) Miranda, K. M.; Katori, T.; Torres de Holding, C. L.; Thomas, L.; Ridnour, L. A.; McLendon, W. J.; Cologna, S. M.; Dutton, A. S.; Champion, H. C.; Mancardi, D.; Tocchetti, C. G.; Saavedra, J. E.; Keefer, L. K.; Houk, K. N.; Fukuto, J. M.; Kass, D. A.; Paolocci, N.; Wink, D. A. *J. Med. Chem.* **2005**, *48*, 8220−8228.

(17) Salmon, D. J.; Torres de Holding, C. L.; Thomas, L.; Peterson, K. V.; Goodman, G. P.; Saavedra, J. E.; Srinivasan, A.; Davies, K. M.; Keefer, L. K.; Miranda, K. M. *Inorg. Chem.* **2011**, *50*, 3262−3270.

(18) Andrei, D.; Salmon, D. J.; Donzelli, S.; Wahab, A.; Klose, J. R.; Citro, M. L.; Saavedra, J. E.; Wink, D. A.; Miranda, K. M.; Keefer, L. K. *J. Am. Chem. Soc.* **2010**, *132*, 16526−16532.

(19) Basudhar, D.; Bharadwaj, G.; Cheng, R. Y.; Jain, S.; Shi, S.; Heinecke, J. L.; Holland, R. J.; Ridnour, L. A.; Caceres, V. M.; Spadari-Bratfisch, R. C.; Paolocci, N.; Velázquez-Martínez, C. A.; Wink, D. A.; Miranda, K. M. *J. Med. Chem.* **2013**, *56*, 7804−7820.

(20) Corrie, J. E. T.; Kirby, G. W.; Mackinnon, J. W. M. *J. Chem. Soc., Perkin Trans. 1* **1985**, 883−886.

(21) Cohen, A. D.; Zeng, B.-B.; King, S. B.; Toscano, J. P. *J. Am. Chem. Soc.* **2003**, *125*, 1444−1445.

(22) Evans, A. S.; Cohen, A. D.; Gurard-Levin, Z. A.; Kebede, N.; Celius, T. C.; Miceli, A. P.; Toscano, J. P. *Can. J. Chem.* **2011**, *89*, 130−138.

(23) Sutton, A. D.; Williamson, M.; Weismiller, H.; Toscano, J. P. *Org. Lett.* **2012**, *14*, 472−475.

(24) Mitroka, S.; Shoman, M. E.; DuMond, J. F.; Bellavia, L.; Aly, O. M.; Abdel-Aziz, M.; Kim-Shapiro, D. B.; King, S. B. *J. Med. Chem.* **2013**, *56*, 6583−6592.

(25) Shoman, M. E.; DuMond, J. F.; Isbell, T. S.; Crawford, J. H.; Brandon, A.; Honovar, J.; Vitturi, D. A.; White, C. R.; Patel, R. P.; King, S. B. *J. Med. Chem.* **2011**, *54*, 1059−1070.

(26) Bodor, N.; Buchwald, P. *Retrometabolic Drug Design and Targeting*; John Wiley & Sons: Hoboken, 2012.

(27) Guthrie, D. A.; Kim, N. Y.; Siegler, M. A.; Moore, C. D.; Toscano, J. P. *J. Am. Chem. Soc.* **2012**, *134*, 1962−1965.

(28) Guthrie, D. A.; Nourian, S.; Takahashi, C. G.; Toscano, J. P. *J. Org. Chem.* **2015**, DOI: 10.1021/jo5023316.

(29) Higashi, Y.; Jitsuiki, D.; Chayama, K.; Yoshizumi, M. *Recent Pat. Cardiovasc. Drug Discovery* **2006**, *1*, 85−93.

(30) Watanabe, T.; Tahara, M.; Todo, S. *Cardiovasc. Ther.* **2008**, *26*, 101−114.

(31) Watanabe, K.; Morinaka, Y.; Iseki, K.; Watanabe, T.; Yuki, S.; Nishi, H. *Redox Rep.* **2003**, *8*, 151−155.

(32) Doyle, M. P.; Mahapatro, S. N.; Broene, R. D.; Guy, J. K. *J. Am. Chem. Soc.* **1988**, *110*, 593−599.

(33) Wong, P. S. Y.; Hyun, J.; Fukuto, J. M.; Shirota, F. N.; DeMaster, E. G.; Shoeman, D. W.; Nagasawa, H. T. *Biochemistry* **1998**, *37*, 5362−5371.

(34) Sandoval, D.; Frazier, C. P.; Bugarin, A.; Read de Alaniz, J. *J. Am. Chem. Soc.* **2012**, *134*, 18948−18951.

(35) Baidya, M.; Griffin, K. A.; Yamamoto, H. *J. Am. Chem. Soc.* **2012**, *134*, 18566−18569.

(36) Palmer, L. I.; Frazier, C. P.; Read de Alaniz, J. *Synthesis* **2014**, *46*, 269−280.

(37) Nagasawa, H. T.; DeMaster, E. G.; Redfern, B.; Shirota, F. N.; Goon, D. J. W. *J. Med. Chem.* **1990**, *33*, 3120−3122.

(38) DeMaster, E. G.; Redfern, B.; Nagasawa, H. T. *Biochem. Pharmacol.* **1998**, *55*, 2007−2015.

(39) Deb, M. L.; Bhuyan, P. J. *Tetrahedron Lett.* **2005**, *46*, 6453−6456.

(40) Reisz, J. A.; Klorig, E. B.; Wright, M. W.; King, S. B. *Org. Lett.* **2009**, *11*, 2719−2721.

(41) Reisz, J. A.; Zink, C. N.; King, S. B. *J. Am. Chem. Soc.* **2011**, *133*, 11675−11685.

(42) Miranda, K. M.; Paolocci, N.; Katori, T.; Thomas, D. D.; Ford, E.; Bartberger, M. D.; Espey, M. G.; Kass, D. A.; Feelisch, M.; Fukuto, J. M.; Wink, D. A. *Proc. Natl. Acad. Sci. U.S.A.* **2003**, *100*, 9196−9201.

(43) Shao, Y.; Molnar, L. F.; Jung, Y.; Kussmann, J.; Ochsenfeld, C.; Brown, S. T.; Gilbert, A. T. B.; Slipchenko, L. V.; Levchenko, S. V.; O'Neill, D. P.; DiStasio, R. A., Jr.; Lochan, R. C.; Wang, T.; Beran, G. J.

DOI: 10.1021/jo502330w
J. Org. Chem. 2015, 80, 1338−1348

O.; Besley, N. A.; Herbert, J. M.; Lin, C. Y.; Van Voorhis, T.; Chien, S. H.; Sodt, A.; Steele, R. P.; Rassolov, V. A.; Maslen, P. E.; Korambath, P. P.; Adamson, R. D.; Austin, B.; Baker, J.; Byrd, E. F. C.; Dachsel, H.; Doerksen, R. J.; Dreuw, A.; Dunietz, B. D.; Dutoi, A. D.; Furlani, T. R.; Gwaltney, S. R.; Heyden, A.; Hirata, S.; Hsu, C.-P.; Kedziora, G.; Khalliulin, R. Z.; Klunzinger, P.; Lee, A. M.; Lee, M. S.; Liang, W. Z.; Lotan, I.; Nair, N.; Peters, B.; Proynov, E. I.; Pieniazek, P. A.; Rhee, Y. M.; Ritchie, J.; Rosta, E.; Sherrill, C. D.; Simmonett, A. C.; Subotnik, J. E.; Woodcock, H. L., III; Zhang, W.; Bell, A. T.; Chakraborty, A. K.; Chipman, D. M.; Keil, F. J.; Warshel, A.; Hehre, W. J.; Schaefer, H. F.; Kong, J.; Krylov, A. I.; Gill, P. M. W.; Head-Gordon, M. *Phys. Chem. Chem. Phys.* **2006**, *8*, 3172−3191.

(44) Pérez-González, A.; Galano, A. *J. Phys. Chem. B* **2012**, *116*, 1180−1188.

(45) Ono, S.; Okazaki, K.; Sakurai, M.; Inoue, Y. *J. Phys. Chem. A* **1997**, *101*, 3769−3775.

(46) Lin, M.; Katsumura, Y.; Hata, K.; Muroya, Y.; Nakagawa, K. *J. Photochem. Photobiol. B: Biol.* **2007**, *89*, 36−43.

(47) Pérez-González, A.; Galano, A. *J. Phys. Chem. B* **2011**, *115*, 1306−1314.

(48) King, S. B.; Nagasawa, H. T. *Methods Enzymol.* **1999**, *301*, 211−220.

(49) Katrizky, A. R.; Barczynski, P.; Ostercamp, D. L. *J. Chem. Soc., Perkin Trans. 2* **1987**, 969−975.

(50) Kosower, E. M.; Pazhenchevsky, B. *J. Am. Chem. Soc.* **1980**, *102*, 4983−4993.

(51) Li, M.; Liu, C.-L.; Yang, J.-C.; Zhang, J.-B.; Li, Z.-N.; Zhang, H.; Li, Z.-M. *J. Agric. Food Chem.* **2010**, *58*, 2664−2667.

(52) Janin, Y. L.; Huel, C.; Flad, G.; Thirot, S. *Eur. J. Org. Chem.* **2002**, 1763−1769.

(53) Armstrong, A.; Jones, L. H.; Knight, J. D.; Kelsey, R. D. *Org. Lett.* **2005**, *7*, 713−716.

DOI: 10.1021/jo502330w
J. Org. Chem. 2015, 80, 1338−1348